Copper supported on mixed alumina/gallium oxide pillared α-tin phosphate for De-NO_x applications

P. Braos-García, J. Santamaría-González, P. Maireles-Torres, E. Rodríguez-Castellón and A. Jiménez-López*

Departamento de Química Inorgánica, Cristalografía y Mineralogía, Facultad de Ciencias, Universidad de Málaga, Campus de Teatinos, 29071 Málaga, Spain.
E-mail: ajimenezl@uma.es

Received 18th July 2001
First published as an Advance Article on the web 8th November 2001

Alumina- and mixed alumina/gallium oxide-pillared α-tin phosphate have been impregnated with different amounts of copper *via* the incipient wetness method. Their characterization by X-ray photoelectron spectroscopy, H_2 temperature-programmed reduction and NO temperature-programmed desorption has allowed to gain insight into the nature of the copper species. These are present as small CuO clusters (not detectable by XRD) as well as forming part of spinel-like structures. NO-TPD studies show that only NO is desorbed from all the catalysts. Ga_3Al_{11}-SnP with 4.9 wt% Cu interacts most strongly with NO and this catalyst exhibits the highest degree of reduction of Cu^{2+} to Cu^{+} after the catalytic reaction. The catalysts are active for the selective catalytic reduction (SCR) of nitric oxide with propane in the presence of excess oxygen.

Introduction

Currently, nitrogen oxides (NO_x) constitute an important environmental problem which is facing more restrictive regulation. NO_x gases are mainly emitted in high temperature combustion processes, both from stationary and automotive sources. Selective catalytic reduction (SCR) is a very interesting alternative for the abatement of NO from combustion sources.

Cu-ZSM-5 is very active for SCR of NO by hydrocarbons, in the presence of oxygen,[1] but lacks durability because it suffers from high deactivation in engine tests. This deactivation process has been attributed either to the presence of water and SO_2 in the gas effluents,[2,3] or to zeolite dealumination, taking place at high temperatures and favouring the concomitant migration of active species to sites not accessible to the reactant molecules.[4] A solution could be the use of more thermally stable supports. Alumina and modified aluminas, used as carriers, are shown to facilitate the dispersion of the active metal, and exhibit good performances for the SCR of NO.[5–7]

On the other hand, pillared layered solids can also be employed as carriers, since the presence of nanoparticles of alumina might increase the dispersion of the active phase. This family of porous materials can be considered as two-dimensional zeolite-like structures, and are obtained from layered hosts (clays, metal(IV) phosphates, *etc.*) by cationic exchange with inorganic polyhydroxo-cations, and subsequent thermal treatment which gives rise to the corresponding oxide nanoparticles, which permanently prop apart the layers creating zeolite-like interlayer and interpillar spaces. Solids with high surface areas and acidity can thus be prepared.[8,9] Pillared materials prepared from lamellar α-metal(IV) phosphates have already been demonstrated to be active in several catalytic reactions,[10–14] exhibiting, for instance, a high thermal stability in oxidative catalysis performed at temperatures as high as 500 °C.

The present work is focused on the use of copper supported on alumina and mixed alumina/gallium oxide-pillared tin phosphates as catalysts in the SCR of NO with propane as reducing agent in an excess of oxygen, and the evaluation of the effect of the nature of copper species, degree of dispersion and reducibility on the catalytic performance.

Results and discussion

Characterization of catalysts

XRD studies indicate that the alumina- and mixed alumina/gallium oxide-pillared tin phosphates, used as supports, are amorphous solids after calcination at 500 °C, reflecting the absence of long-range order. Only the Ga_3Al_{11}-SnP material shows a diffraction signal corresponding to a basal spacing of *ca.* 20 Å. The supports possess S_{BET} values between 87 and 178 $m^2\ g^{-1}$, being mesoporous solids with a certain contribution of micropores (Table 1). The mesoporous nature of these materials might be attributed to platelet stacking or end–end particle interactions, while the microporosity arises from the interlayer cavities induced by pillaring. Furthermore, these supports are acid solids, with total acidity per surface area unit measured by NH_3-TPD, ranging from 3.0 to 5.9 μmol $NH_3\ m^{-2}$ and increasing, as expected, with the gallium content, owing to the higher acidity of this element relative to Al(III).

In Table 1, it can be seen that upon the incorporation of copper oxide, in all cases, the specific surface area values decrease. Thus, catalysts prepared using Ga_3Al_{11}-SnP as support, show a reduction in surface area of between 45 and

Green Context

While the treatment of emissions is not part of green chemistry *per se* we must recognise that the effective treatment of inevitable process emissions is important. This should involve minimal inputs in terms of materials and energy as well as being highly efficient and not creating secondary pollutants. Here we can read about a new material for the selective catalytic reduction of nitric oxide and propane. The paper also reports important data on the preparation and characterisation of these useful materials. Knowledge about the redox properties of the active phase should prove to be especially useful potentially in synthetic as well as destructive applications. ***JHC***

DOI: 10.1039/b106392h

58%, increasing with the amount of copper supported. This reduction in area can be mainly attributed to the blockage of micro- and meso-pores by CuO particles resulting from the impregnation process. The Ga_6Al_7-SnP-Cu4.9 catalyst shows the minimum decrease in its S_{BET} value, probably due to its mesoporous nature.

Considering the acid characteristics of catalysts, they have a total acidity higher than those of the supports, indicating that copper oxide particles can act as Lewis acid sites. However, there is no clear relationship between the acidity and the amount of copper added, thus suggesting that the aggregation state of the supported CuO will affect the resulting acidity.

X-Ray photoelectron spectroscopy allows detection of the existence of a fraction of Cu^{2+} ions forming part of a spinel-like structure. The XPS spectrum in the region of Cu 2p (Fig. 1) exhibits a large and asymmetric peak with a maximum at 932.0–932.5 eV, assigned to CuO,[15] accompanied by a shoulder at 934.5–935.0 eV, attributed to Cu^{2+} in spinel-like structure occupying octahedral sites.[16,17] This latter coordination contrasts with that in bulk spinel where copper is predominantly in a tetrahedral environment.[18] Table 2 details the percentage of Cu^{2+} in each environment. The amount of spinel-like copper increases with copper loading, as can be seen for catalysts on Ga_3Al_{11}-SnP with variable copper contents. In the same way, the percentage of copper in the spinel-like structure of catalysts with 4.9 wt% Cu slightly decreases with gallium content, ranging from 21.3 to 19.2% for catalysts containing gallium, whereas a value of 32.7% is reached for the Al-SnP-Cu4.9 catalyst. These results suggest that diffusion of Cu^{2+} ions into the mixed Ga/Al oxide nanostructures is more difficult; perhaps the higher ionic potential of gallium ions hinders the diffusion of Cu^{2+} ions in such oxide nanoparticles.

The surface Sn/Cu atomic ratios, calculated from XPS, decrease with copper content, and in all cases they are lower than the corresponding bulk values (Table 2). This behaviour is typical of supported catalysts with a low degree of coverage, and reflects dispersion of the active phase on the supports. This latter assumption is supported by the absence in the corresponding XRD patterns of peaks at 2.52 and 2.32 Å, typical of CuO crystallites, or a peak at 2.44 Å, attributable to $CuAl_2O_4$.[5] The H_2-TPR curves of the family of copper supported Ga_3Al_{11}-SnP catalysts (Fig. 2) show that the catalyst with the lowest copper loading, 2.5 wt%, has a reduction profile consisting of a very broad band, extended from 180 to 425 °C. This large reduction interval indicates that Cu(II) species are located in many different chemical environments, while the high reduction temperatures probably reveals a strong interaction with the support surface. With increasing copper content, a peak the maximum of which shifts to lower temperatures, is observed, indicating that the reduction process of Cu^{2+} to Cu^0 becomes easier.[6] Taking into account that the H_2-TPR curve of bulk CuO displays a single reduction peak at lower temperature (220 °C), and, on the other hand, that the reduction temperature decreases as the particle size of CuO increases,[18] it seems that a good dispersion is achieved on the Ga_3Al_{11}-SnP support, even for high copper loading. Concerning the shoulder appearing in all catalysts between 300 and 400 °C, this could be attributed to the reduction of Cu^{2+} forming spinel-like structures, already detected by XPS, which, according to literature reports, are more difficult to reduce.[5]

For catalysts with 4.9 wt% of copper supported on the different supports (Fig. 3), a peak is observed, the temperature of maximum intensity of which varies from 241 °C for Ga_3Al_{11}-SnP-Cu4.9 to 285 °C for $GaAl_{13}$-SnP-Cu4.9. Furthermore, a large shoulder is more pronounced upon increasing the percentage of Cu^{2+} in spinel-like structure, in accord with the XPS data. Among catalysts with 4.9 wt% of copper, that supported on Ga_3Al_{11}-SnP is the most easily reducible.

An NO temperature-programmed desorption study of catalysts with 4.9 wt% of copper (Fig. 4) indicates that, in all cases, only NO is desorbed. Similar results have already been reported for copper catalysts supported on mordenite, but, in this latter case, NO and O_2 were detected at high temperatures due to the

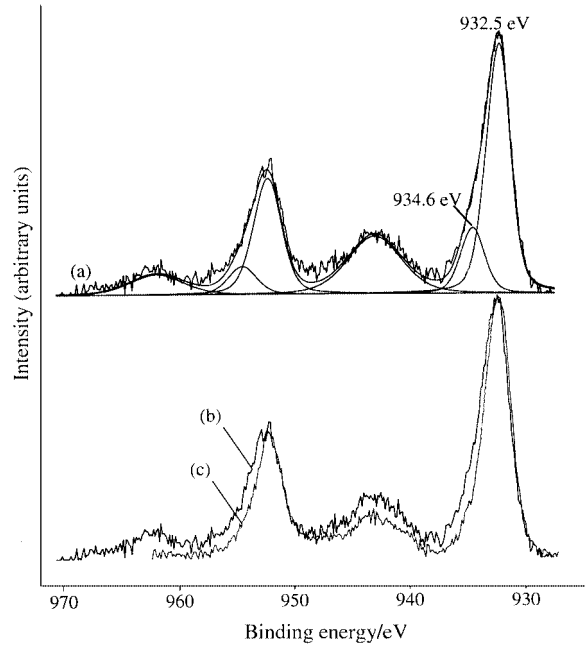

Fig. 1 Cu 2p core level X-ray photoelectron spectra for Ga_3Al_{11}-SnP-Cu4.9: (a) fresh (deconvoluted), (b) fresh and (c) spent catalyst.

Table 1 Chemical composition, textural and acidic properties of alumina and mixed alumina/gallium oxide pillared tin phosphate supports and the corresponding copper containing catalysts

Sample	Chemical composition (wt%) Al_2O_3	Ga_2O_3	S_{BET}/m² g⁻¹	V_μ[a]/cm³ g⁻¹	Total acidity/ μmol NH_3 m⁻²
Al-SnP	18.9	—	164	0.075	3.0
Al-SnP-Cu2.5			76	0.027	5.2
Al-SnP-Cu4.9			71	0.024	5.8
$GaAl_{13}$-SnP	16.7	3.4	178	0.068	3.2
$GaAl_{13}$-SnP-Cu4.9			86	0.028	10.1
Ga_3Al_{11}-SnP	13.7	11.9	174	0.134	4.9
Ga_3Al_{11}-SnP-Cu2.5			95	0.034	8.3
Ga_3Al_{11}-SnP-Cu4.9			86	0.032	7.9
Ga_3Al_{11}-SnP-Cu7.1			74	0.029	11.5
Ga_3Al_{11}-SnP-Cu9.2			73	0.029	9.3
Ga_6Al_7-SnP	3.7	26.5	87	0.036	5.9
Ga_6Al_7-SnP-Cu4.9			70	0.024	9.6

[a] Micropore volume obtained using the Dubinin–Radushkevich equation.

Table 2 XPS data of copper supported catalysts

Sample	Cu $2p_{3/2}$ E_b/eV[a]		%Cu in spinel-like structure	Sn/Cu Atomic ratio		Cu $2p_{3/2}$/satellite area ratio (%)	
				Surface[a]	Bulk	Fresh	Spent
Al-SnP-Cu2.5	932.5	934.8	23.0	1.62	5.02	1.75	1.95
Al-SnP-Cu4.9	932.4	934.8	32.7	1.14	2.51	1.27	3.21
$GaAl_{13}$-SnP-Cu4.9	932.5	935.0	21.3	1.79	2.53	1.73	2.87
Ga_3Al_{11}-SnP-Cu2.5	932.0	934.6	18.0	2.56	4.30	1.54	2.24
Ga_3Al_{11}-SnP-Cu4.9	932.5	934.6	20.4	1.60	2.15	1.93	3.23
Ga_3Al_{11}-SnP-Cu7.1	932.4	934.5	26.8	1.02	1.45	1.57	2.91
Ga_3Al_{11}-SnP-Cu9.2	932.3	934.5	37.5	0.98	1.10	1.33	2.34
Ga_6Al_7-SnP-Cu4.9	932.5	935.0	19.2	2.24	2.21	1.39	2.26

[a] From XPS analysis.

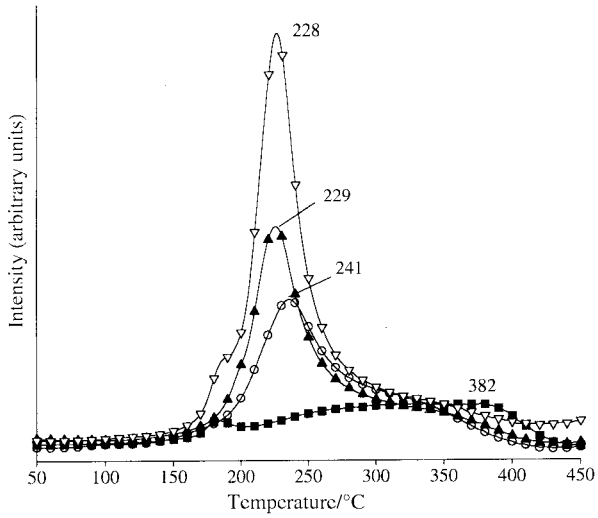

Fig. 2 H_2-TPR curves of copper supported catalysts on Ga_3Al_{11}-SnP: (■) 2.5, (○) 4.9, (▲) 7.1 and (▽) 9.2 wt% of copper.

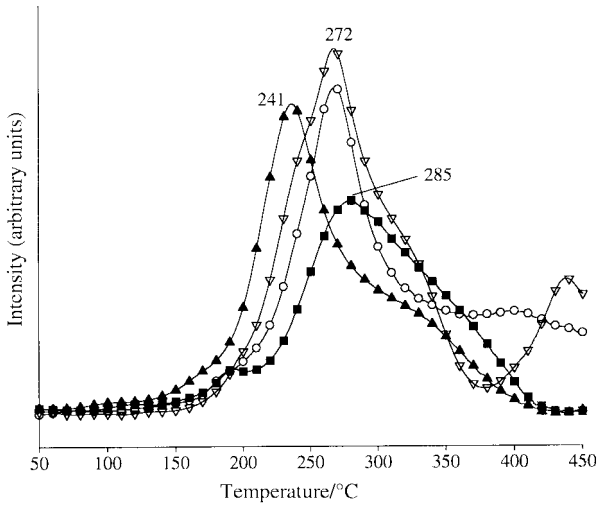

Fig. 3 H_2-TPR curves of copper supported catalysts with 4.9 wt% of copper on: (○) Al-SnP, (■) $GaAl_{13}$-SnP, (▲) Ga_3Al_{11}-SnP and (▽) Ga_6Al_7-SnP.

decomposition of NO_3^- and NO_2^- adsorbed species.[19] However, this behaviour differs from that found for copper-exchanged ZSM-5 zeolite, where N_2O was also observed at low temperatures.[20] Regarding the amount of NO and its desorption temperature range, they seem to depend on the type of support. Thus, the highest amount of NO desorbed is found for the Al-SnP-Cu4.9 catalyst, which exhibits the lowest surface Sn/Cu atomic ratio, 1.14 (Table 2), and hence the maximum amount of

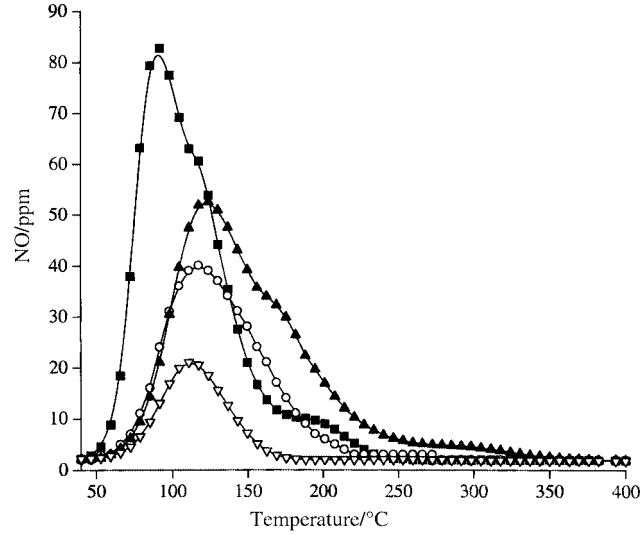

Fig. 4 NO-TPD curves of copper supported catalysts with 4.9 wt% of copper on: (■) Al-SnP, (○) $GaAl_{13}$-SnP, (▲) Ga_3Al_{11}-SnP and (▽) Ga_6Al_7-SnP.

surface copper. However, its interaction with NO molecules is very weak, since desorption occurs at low temperatures, as demonstrated by the maxima at 92 and 117 °C. Among gallium containing catalysts, Ga_3Al_{11}-SnP-Cu4.9 retains the highest amount of NO, and its desorption occurs at higher temperatures (123 and 169 °C), which can be explained by a good metal oxide dispersion and, furthermore, its special interaction with the substrate could favour the establishment of a strong linkage with NO molecules.

Catalytic results

It has previously been reported that for a given feed (oxygen, hydrocarbon and NO), the catalytic performance in the selective catalytic reduction of NO depends on both the type of hydrocarbon and the active species.[21] In order to evaluate the catalytic behavior of this family of copper-based catalysts we have chosen propane as the reducing agent. Furthermore, the presence of oxygen in excess is required since there are two chemical reactions competing for this molecule [eqn. (1) and (2)]:

$$C_3H_8 + 2\ NO + 4\ O_2 \rightarrow N_2 + 3\ CO_2 + 4\ H_2O \quad (1)$$

$$C_3H_8 + 5\ O_2 \rightarrow 3\ CO_2 + 4\ H_2O \quad (2)$$

Under our experimental conditions, the reaction products were N_2, NO_2 and CO_2, whereas neither N_2O nor CO were detected. The study of the NO conversion as a function of the reaction temperature for catalysts obtained from the Ga_3Al_{11}-SnP support (Fig. 5), shows that conversion always increases

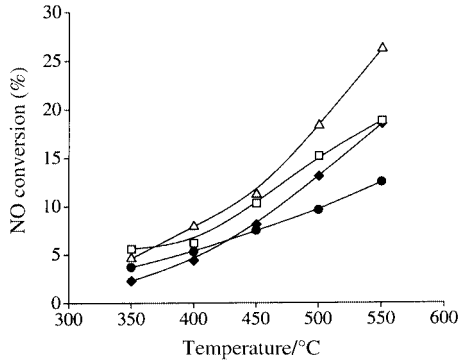

Fig. 5 NO conversion as a function of the reaction temperature of copper supported on Ga_3Al_{11}-SnP: (●) 2.5, (△) 4.9, (◆) 7.1 and (□) 9.2 wt% of copper. Experimental conditions: NO = 1000 ppm, C_3H_8 = 1000 ppm, 2.5 vol% O_2, flow rate = 150 cm^3 min^{-1}, space velocity = 60000 cm^3 g^{-1} h^{-1}.

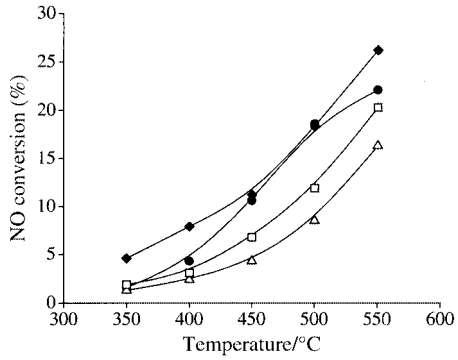

Fig. 6 NO conversion as a function of the reaction temperature of copper supported catalysts with 4.9 wt% of copper on: (●) Al-SnP, (△) $GaAl_{13}$-SnP (◆) Ga_3Al_{11}-SnP and (□) Ga_6Al_7-SnP.

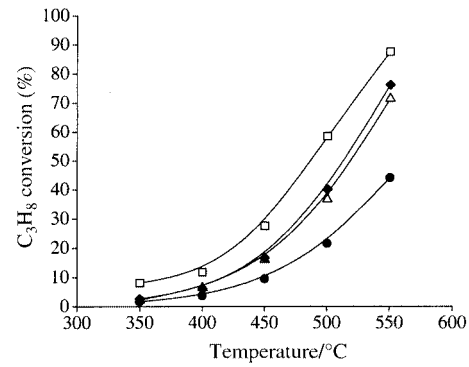

Fig. 7 Propane conversion as a function of the reaction temperature of copper supported on Ga_3Al_{11}-SnP: (●) 2.5, (△) 4.9, (◆) 7.1 and (□) 9.2 wt% of copper.

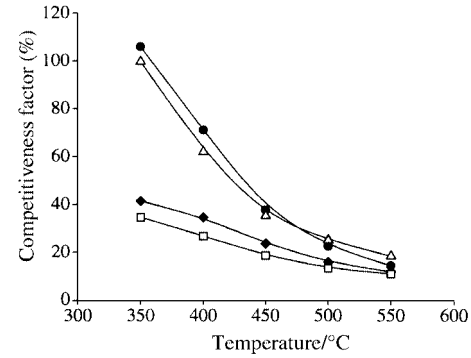

Fig. 8 Competitiveness factor of propane conversion as a function of the reaction temperature of copper supported on Ga_3Al_{11}-SnP: (●) 2.5, (△) 4.9, (◆) 7.1 and (□) 9.2 wt% of copper.

with temperature. It also depends on the copper content, the catalyst with 4.9 wt% of copper being the more active at 550 °C, with a conversion of 26.2%. The catalyst with 2.5 wt% Cu presents the lowest catalytic activity, which can be rationalized by its H_2-TPR data which point to the presence of less reducible copper species, and therefore the formation of the active species Cu^+ in this catalytic reaction is more difficult. Among the other catalysts derived from Ga_3Al_{11}-SnP, with a similar temperature for the maximum of reduction, that with 4.9 wt% of copper shows the highest amount of exposed copper oxide. Moreover, taking into account that increasing the copper loading leads both to an increase in the spinel percentage (difficult to reduce) and an increase in CuO particle size, the highest activity of catalyst Ga_3Al_{11}-SnP-Cu4.9 in the temperautre range 400–550 °C can be explained on the basis of a higher presence of surface Cu^{2+} species. Analogous results have been described in the literature; thus, Park and Ledford[22] found a decrease in catalytic activity when increasing the amount of copper supported on alumina, that is, as isolated copper species increasingly are replaced by discrete CuO particles.

Considering the influence of the support in the SCR of NO for a fixed Cu loading, 4.9 wt% (Fig. 6), it can be appreciated that the most active catalyst, in all range of temperatures studied, again is Ga_3Al_{11}-SnP-Cu4.9. These results agree well with both the NO-TPD data, which evidenced the strongest interaction of this catalyst with the NO molecules, and its lower H_2 reduction temperature. Although peaks in H_2-TPR curves are assigned to total Cu^{2+} to Cu^0 reduction process, it is possible, under our experimental conditions, that only a partial reduction process takes place, leading to Cu^+ ions, which are thought to be the active species in this catalytic reaction, due to their capacity to generate dinitrosyl complexes.[23,24]

Regarding the propane conversion, in Fig. 7 it can be observed that, for catalysts derived from Ga_3Al_{11}-SnP, this also increases as the reaction temperature is increased, ranging, at 550 °C, between 43 and 85%. Therefore, it can be argued that upon increasing the temperature the combustion reaction of propane is favoured relative to the selective reduction of NO. Similar conversion percentages have been obtained on catalysts with 4.9 wt% of copper.

In all cases, a decay in the competitiveness factor with temperature can be observed, the values ranging between 11 and 18% for catalysts derived from Ga_3Al_{11}-SnP with variable copper loadings (Fig. 8), and between 10 and 22% for catalysts on different supports with the same copper content (4.9 wt%). The most active catalyst, Ga_3Al_{11}-SnP-Cu4.9, shows a competitiveness value of 18.2% at 550 °C..

The catalytic activity of these copper oxide impregnated materials are similar to those described for alumina pillared zirconium phosphate impregnated with copper oxide.[25] However, the catalysts studied in the present work are more active than those based on copper oxide supported over alumina pillared montmorillonite.[26] They are also more active than copper oxide supported on alumina catalysts[27] which indicates that the dispersion of alumina, as nanoparticles in the interlayer region of layered tetravalent metal phosphates, favours the formation of small CuO particles, *i.e.* it leads to a better dispersion of the active phase.

Nevertheless, a copper containing ZSM-5 catalyst (2.8 wt% of copper), under the same reaction conditions, exhibits a NO conversion close to 100% with a TOF value of 15.62×10^{-4} molecules of NO per Cu atom and also is almost seven times higher than the most active of our catalysts, 2.30×10^{-4} molecules of NO per Cu atom (Table 3). The low TOF values can be explained taking into account that, according to the proposed mechanism for the NO SCR with propane, not only a presence of Cu^{2+} ions easily reducible to Cu^+ is required, but also the activation of the reducing agent molecule (propane) on

Table 3 Catalytic properties of copper supported catalysts in the SCR of NO

Catalyst	NO conversion (%)	C_3H_8 conversion (%)	Activity/ μmol g_{cat}^{-1} s^{-1}	10^4 TOF/$molec_{NO}$ at_{Cu}^{-1} s^{-1}
Al-SnP-Cu2.5	7.9	44.4	0.05	1.35
Al-SnP-Cu4.9	22.1	90.2	0.15	1.94
$GaAl_{13}$-SnP-Cu4.9	16.3	51.1	0.11	1.43
Ga_3Al_{11}-SnP-Cu2.5	12.5	44.1	0.09	2.13
Ga_3Al_{11}-SnP-Cu4.9	26.2	71.4	0.18	2.30
Ga_3Al_{11}-SnP-Cu7.1	18.5	76.2	0.13	1.12
Ga_3Al_{11}-SnP-Cu9.2	18.8	87.6	0.13	0.89
Ga_6Al_7-SnP-Cu4.9	20.3	42.5	0.14	1.78
Cu-ZSM5-Cu2.8	86.6	98.9	0.59	15.62

the acidic Brönsted sites of support.[26] These acid sites are scarce in these materials the most abundant being of Lewis type.

The spent catalysts after the NO SCR were studied by XPS in order to determine the nature of the copper species after catalysis. Cu 2p spectra corresponding to Cu(II) species are characterised by a doublet, Cu $2p_{3/2}$ at *ca.* 932.4 eV and Cu $2p_{1/2}$ at *ca.* 952.4 eV signals, both accompanied by weak and wider satellite peaks at *ca.* 943.1 and 962.0 eV, respectively. From Fig. 1, significant differences between the spectra before and after the catalytic reaction are observed (Table 2). Thus, in spent catalysts, the satellite peak corresponding to Cu $2p_{3/2}$ diminishes, while that of Cu $2p_{1/2}$ almost disappears. By comparing the integrated area ratios of the Cu $2p_{3/2}$ and satellite bands, an increase is observed after the catalytic reaction. Since copper species with lower oxidation state (0 or 1+) only show the main peaks, it can be deduced that these increments of integrated area ratios are caused by the disappearance of Cu^{2+} ions due to its partial reduction to generate Cu^{+} during SCR of NO. It is noteworthy that the most active catalyst, Ga_3Al_{11}-SnP-Cu4.9, shows the highest area ratio, indicating that it easily forms the Cu^{2+}/Cu^{+} pair, required in this catalytic reaction.

The most active catalyst, Ga_3Al_{11}-SnP-Cu4.9, has been chosen to evaluate the influence of parameters such as the partial oxygen pressure, and the NO and propane concentrations in the feed on the catalytic performance. Fig. 9 shows the effect of oxygen addition; in the absence of oxygen, the NO conversion is 11%, increasing to 24% as the oxygen concentration is raised to 0.5 vol%. However, further increase does not affect the NO conversion, which remains almost constant and near to 21% and hence the reaction is zero order with respect to oxygen. These results are in agreement with those reported in the literature for copper catalysts based on alumina pillared zirconium phosphate[25] and Co-ZSM-5.[25]

Concerning propane conversion, an enhancement is observed for oxygen partial pressures above 1.5 vol%, the oxidation reaction of propane being considerably favoured with the conversion value stabilized around 71%. Although an excess of oxygen implies a higher degree of oxidation of propane, and thus, a lower competitiveness factor, this is necessary, since, in addition to preventing the formation of carbonaceous deposits, which would deactivate the catalyst, it favours the reoxidation of Cu(I) to Cu(II), and the formation of NO_2 and oxygenated products with propane.[28]

Fig. 10, shows NO and propane conversions as a function of the propane concentration in the feed. It can be observed that the NO conversion is enhanced up to 44%. From a plot of log (rate of reduction) *vs.* log (partial pressure propane in feed) a reaction order of this reactant of 0.51 is found.

The evolution of NO and propane conversions as a function of the NO composition in the feed (Fig. 11) shows a decay in the NO conversion, although as the propane conversion remains almost constant, the competitiveness factor increases. The order of reaction with respect to NO is 0.44, which is also near to those found using other catalytic systems.

Finally, the influence of the space velocity (*F*/*W*) on NO and propane conversions has been studied. From Fig. 12, it can be observed that NO conversion decreases from 30 to 14% upon increasing this parameter from 20000 to 120000 $cm^3\,h^{-1}\,g^{-1}$. However, although the propane conversion is much more affected, diminishing from 89 to 40%, this decrease is almost parallel to that of NO conversion, and so the competitiveness factor scarcely changes with space velocity.

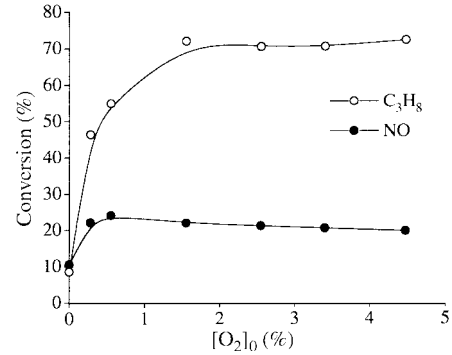

Fig. 9 Effect of the oxygen concentration on the propane and NO conversions for Ga_3Al_{11}-SnP-Cu4.9 catalyst at 550 °C.

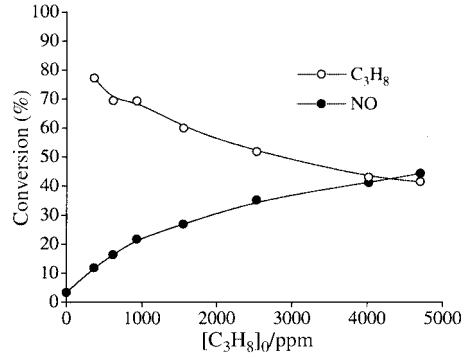

Fig. 10 Variation of the propane and NO conversions with the propane concentration in the feed for Ga_3Al_{11}-SnP-Cu4.9 catalyst at 550 °C.

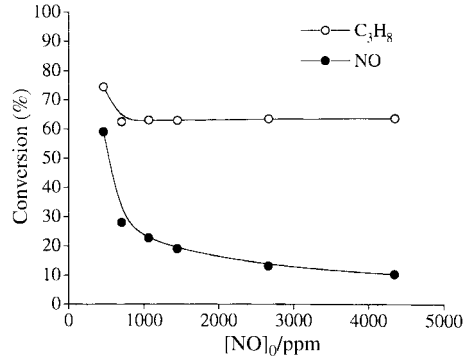

Fig. 11 Dependence of the propane and NO conversions with the NO concentration in the feed for Ga_3Al_{11}-SnP-Cu4.9 catalyst at 550 °C.

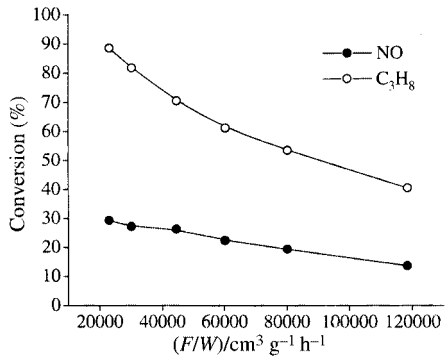

Fig. 12 Variation of the propane and NO conversions as a function of the space velocity for Ga_3Al_{11}-SnP-Cu4.9 catalyst at 550 °C.

In conclusion, copper oxide supported on alumina and mixed alumina/gallium oxide pillared tin phosphate catalysts exhibit a moderate activity in the selective catalytic reduction of NO with propane. Among them, catalyst Ga_3Al_{11}-SnP-Cu4.9 is the most active because it combines suitable conditions, such as high dispersion of the active phase and good reducibility. The full characterisation of the catalysts obtained in this work, especially relating to the redox properties of the active phase is of great interest when considering the use of these catalysts for the SCR of NO with other reducing agents such as ammonia.

Experimental

Preparation of catalysts

A series of porous materials based on alumina and mixed alumina/gallium oxide (with Al/Ga molar ratios of 1/13, 3/11, and 6/7) pillared α-tin phosphates have been synthesised as described elsewhere,[29] and calcined in air at 500 °C for 8 h. These supports are designated as Al-SnP, $GaAl_{13}$-SnP, Ga_3Al_{11}-SnP and Ga_6Al_7-SnP.

These solids were then impregnated with copper species by using the incipient wetness method with aqueous copper acetate solutions followed by solvent evaporation in air at 60 °C, and calcination at 500 °C for 4 h. In this manner, catalysts with different copper loading have been prepared. The weight percentage of copper present on each catalyst is indicated after the name of the support (for instance AlSnP-Cu4.9 corresponds to 4.9 wt% of Cu on the AlSnP support).

A Cu-ZSM-5 sample, prepared by ion-exchange with copper acetate at room temperature of a synthesized ZSM-5 (Si/Al molar ratio of 13.5, copper content of 2.8 wt% corresponding to an exchange level of 79%), was used as a reference.

Characterization methods

XRD patterns were obtained with a Siemens D501 diffractometer using Cu-Kα radiation and a graphite monochromator. N_2 adsorption–desorption isotherms at 77 K were measured in a conventional volumetric apparatus after outgassing of samples at 200 °C and 10^{-4} Torr overnight. The total acidity of catalysts was elucidated by temperature-programmed desorption of ammonia (NH_3-TPD), between 100 and 500 °C, as previously described.[29]

XPS analyses were carried out with a Physical Electronics 5700 instrument with an Mg-Kα X-ray excitation source ($h\nu$ = 1253.6 eV) and a hemispherical electron analyser. Accurate ± 0.1 eV binding energies were determined with respect to the position of the adventitious C 1s peak at 284.8 eV. The residual pressure in the analysis chamber was maintained below 10^{-9} Torr during data acquisition.

Hydrogen temperature-programmed reduction (H_2-TPR) curves were obtained between 40 and 450 °C, using a H_2/Ar flow (48 cm³ min⁻¹, 10 vol% of H_2) and a heating rate of 10 °C min⁻¹. The water produced in this reaction was eliminated by passing the gas flow through a cold finger (−80 °C). The hydrogen consumption was monitored by an on-line gas chromatograph (Shimadzu 6C-14A) equipped with a TCD. Previously, samples (50 mg) were treated at 500 °C under a O_2/He flow (50 cm³ min⁻¹, 5 vol% of O_2) for 30 min, and then under a helium flow (100 cm³ min⁻¹) for 30 min.

The study of the temperature-programmed desorption of NO (NO-TPD) was carried out using *ca.* 150 mg of catalyst, previously treated at 550 °C under a flow of 70 cm³ min⁻¹ of O_2/He (5 vol% of O_2) for 30 min, and then under a flow of 100 cm³ min⁻¹ of He for 30 min. Once at room temperature, NO adsorption was carried out by passing a flow of 100 cm³ min⁻¹ of 0.05 vol% NO in helium for 30 min. Then, a helium flow of 100 cm³ min⁻¹ was passed until a stable signal of NO was obtained (baseline). Desorption of NO was performed between 40 and 550 °C, with a heating rate of 10 °C min⁻¹, under a helium flow of 100 cm³ min⁻¹. During this process eluted gas was monitored and quantified using an on-line quadrupole mass spectrometer Pfeiffer Balzers OmniStar, equipped with a ChannelTron detector.

The catalytic activities in the SCR of NO were measured using a micro-reactor in a steady-state flow mode. 150 mg of samples (0.3–0.4 mm particle diameter) were packed into a tubular quartz reactor (6 mm i.d.) and plugged with quartz wool. Catalysts were activated at 500 °C (10 °C min⁻¹ heating rate) under a helium flow of 70 cm³ min⁻¹ for 1 h. The reaction mixture was prepared by using four mass-flow controllers and consisted of 1000 ppm NO, 1000 ppm propane and 2.5% O_2 (balanced with helium) with a total flow rate of 150 cm³ min⁻¹. Under these experimental conditions, the space velocity (*F*/*W*) was 60000 cm³ h⁻¹ g⁻¹. The reaction temperature was varied between 350 and 550 °C. An on-line quadrupole mass spectrometer Pfeiffer Balzers OmniStar was used to monitor the gas effluent at each temperature and thus to measure the NO and propane concentration. The activity was obtained on the basis of disappearance of NO fed. The competitiveness factor was calculated as the ratio of mol propane reacted with NO to the total mol propane consumed in the reaction.

Acknowledgements

This research was performed under the contract No. BRPR CT97 0545 of the European Union. We also wish to thank the CICYT (Spain) (Project MAT97-906) for financial support. P.B.G. thanks Junta de Andalucía (Spain) for a fellowship.

References

1 M. Iwamoto and N. Mizuno, *J. Auto Eng.*, 1993, **207**, 23.
2 M. J. Heimrich and M. L. Deviney, *SAE Pap.*, 930736, 1994.
3 J. N. Armor, *Appl. Catal. B*, 1994, **4**, N18.
4 T. Tanabe, T. Iijima, A. Koinai, J. Mizuno, K. Yokota and A. Isoga, *Appl. Catal. B*, 1996, **6**, 145.
5 J. A. Anderson, C. Márquez Álvarez, M. J. López Muñoz, I. Rodríguez Ramos and A. Guerrero Ruiz, *Appl. Catal. B*, 1997, **14**, 189.
6 K. W. Yao, S. Jaenicke, J. Y. Lin and K. L. Tan, *Appl. Catal. B*, 1998, **16**, 291.
7 H. Praliaud, S. Mikhailemko, Z. Chajar and M. Primet, *Appl. Catal. B*, 1998, **16**, 359.
8 *Pillared Layered Structures: Current Trends and Applications*, ed. I. V. Mitchell, Elsevier, London, 1990, pp. 137.
9 P. Olivera-Pastor, P. Maireles-Torres, E. Rodríguez-Castellón, A. Jiménez-López, T. Cassagneau, D. J. Jones and J. Rozière, *Chem. Mater.*, 1996, **8**, 1758.

10 A. Jiménez-López, J. Maza-Rodríguez, E. Rodríguez-Castellón and P. Olivera-Pastor, *J. Mol. Catal. A*, 1996, **108**, 175.
11 F. J. Pérez-Reina, E. Rodríguez-Castellón and A. Jiménez-López, *Langmuir*, 1999, **15**, 8421.
12 J. Mérida-Robles, P. Olivera-Pastor, E. Rodríguez-Castellón and A. Jiménez-López, *J. Catal*., 1997, **169**, 317.
13 J. Mérida-Robles, E. Rodríguez-Castellón and A. Jiménez-López, *J. Mol. Catal. A*, 1999, **145**, 169.
14 B. Solsona, J. M. López-Nieto, M. Alcántara-Rodriguez, E. Rodríguez-Castellón and A. Jiménez-López, *J. Mol. Catal. A*, 2000, **153**, 199.
15 G. Ertl, R. Hierl, H. Knözinger, N. Thiele and H. P. Urbach, *Appl. Surf. Sci*., 1980, **5**, 49.
16 E. C. Marques, M. R. Friedman and D. J. Dahm, *Appl. Catal*., 1985, **19**, 387.
17 P. A. Berger and J. F. Roth, *J. Phys. Chem*., 1967, **71**, 4307.
18 R. M. Friedman, J. J. Freeman and F. W. Lytle, *J. Catal*., 1978, **55**, 10.
19 C. Torre-Abreu, M. F. Ribeiro and G. Delahay, *Appl. Catal. B*, 1997, **14**, 261.
20 Y. Li and J. N. Armor, *Appl. Catal*., 1991, **76**, L1.
21 M. Iwamoto and H. Hamada, *Catal. Today*, 1991, **10**, 57.
22 W. Park and J. S. Ledford, *Appl. Catal. B: Environ*., 1998, **15**, 221.
23 Y. Li and J. N. Armor, *Appl. Catal. B*, 1993, **2**, 239.
24 J. O. Petunchi, G. Stilly and W. K. Hall, *Appl. Catal. B*, 1993, **2**, 303.
25 R. Hernández-Huesca, J. Santamaría-González, P. Braos-García, P. Maireles-Torres, E. Rodríguez-Castellón and A. Jiménez-López, *Appl. Catal. B: Environ*., 2000, **732**, 1.
26 S. Perathoner and A. Vaccari, *Clay Miner*., 1997, **32**, 123.
27 Z. Chajar, M. Primet, H. Praliaud, M. Chevrier, C. Gauthier and L. Mathis, *Appl. Catal. B*, 1994, **4**, 199.
28 J. O. Petunchi and W. K. Hall, *Appl. Catal. B*, 1993, **2**, L17.
29 P. Braos-García, E. Rodríguez-Castellón, P. Maireles-Torres, P. Olivera-Pastor and A. Jiménez-López, *J. Phys. Chem B*, 1998, **102**, 1672.